

The Long Arm of Calculus ***Ethan Berkove and Rich Marchand***

The College Mathematics Journal, November 1998, Volume 29, Number 5,
pp. 376–386.

Ethan Berkove (ae5450@usma.edu) holds a Davies Associateship, which combines teaching at the U.S. Military Academy, West Point, with research at the Army Research Labs. At the University of Michigan he majored in mathematics and Japanese, and his Ph.D. (1996) is from the University of Wisconsin under Alejandro Adem. Besides dabbling in applications of mathematics, he enjoys origami and his favorite application of physics: rock climbing.

Rich Marchand (ar9452@usma.edu), who is also a Davies Associate, teaches mathematics and conducts research in “smart” munitions. He has a B.S. in mathematics with a minor in computer science and certification in secondary mathematics education from Clarion University of Pennsylvania. His Ph.D. (1996) in applied mathematics from the University of Virginia was completed under Irena Lasiecka. Rich enjoys spending time with his wife and two daughters.

At the United States Military Academy our students all have the same curriculum, which includes two semesters of physics and four of mathematics. Recently, while teaching the multivariable course, we decided to develop a coursewide project that would motivate the need for functions of many variables while using basic concepts from physics. We also wanted a nonstandard application of vectors, one that was not of the “projectile shot from a cannon” variety. After consulting with the physics faculty, we decided to conduct a torque analysis of the robot arm on the space shuttle. Much to our surprise, what at first seemed to be a straightforward analysis of a simple model became more and more interesting the deeper we delved—and multivariable calculus provided just the tools we needed.

Modeling the Long Arm

The space shuttle’s robot arm is designed to snag an orbiting satellite and move it to the shuttle bay. We model the arm as two hinged segments of different lengths, $l_1 > l_2$, as shown in Figure 1. Three elements contribute to the torque about the primary joint: the masses of the two arm segments and the mass of the satellite. Given a restriction on the admissible torque about the *primary joint*—the joint that connects the robot arm to the shuttle—our goals are to identify the region from which the robot arm can retrieve a satellite and to analyze the return path followed by the two robot arm segments as the satellite is brought into the shuttle bay. Along the way we determine the maximum satellite retrieval distance. The recent fiasco involving the collision of an unmanned supply ship with the MIR space station makes this goal an especially timely topic.

Taking a typical modeling approach, we make some simplifying assumptions. First, we assume that the shuttle, the satellite, and the two segments of the robot arm lie in the same plane, and that the satellite is at rest with respect to the shuttle. The nonplanar generalization is more complicated but does not involve any fundamentally new ideas. We next consider the shuttle’s orbit. If the shuttle and satellite were traveling in a stable orbit, the robot arm and the satellite would be weightless. Then an arbitrarily small force

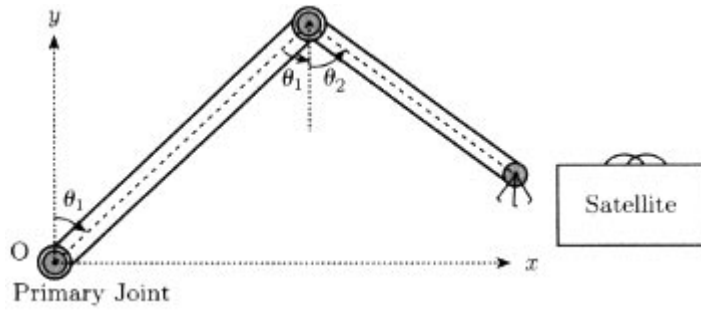


Figure 1. The shuttle arm.

would suffice to retrieve the satellite, and therefore the torque on the primary joint could be kept as small as desired. Thus, from the stable orbit we give the shuttle an additional small constant acceleration, which produces the effect of a weak “phantom gravity,” pulling objects in the opposite direction. By substituting the gravitational acceleration of objects at the surface of the earth, we can apply our analysis to robot arms on earth as well.

We used the following numerical values to generate the graphs in this article. The lengths of the two arm segments are $l_1 = 10.5$ m and $l_2 = 6$ m. Their masses, $m_1 = 90$ kg and $m_2 = 75$ kg, are assumed to be uniformly distributed, so the center of mass of each segment lies at its midpoint. The mass of the satellite is $m_3 = 80$ kg and the constant acceleration due to the “phantom gravity” is $a = 0.4$ m/sec².

The torque about a point O produced by a force \mathbf{F} on a body is given by the vector cross product $\mathbf{r} \times \mathbf{F}$, where \mathbf{r} is the vector from O to the point where the force is applied. We introduce coordinate axes in the plane of our system as indicated in figure 2, so that the phantom gravity forces on the two segments of the robot arm and the satellite are $-(m_i a)\mathbf{j}$, where $1 \leq i \leq 3$. The robot arm segments are assumed to be never more than 180° apart, and we suppose that the short segment never moves clockwise past the long one. We also assume the line segment has a range of motion of 180° . Thus the angles θ_1 and θ_2 are constrained to satisfy $0 \leq \theta_1 + \theta_2 \leq \pi$ and $0 \leq \theta_1 \leq \pi$.

The part of the shuttle bay at which the satellite can be retrieved is taken to be where θ_1 and θ_2 are both zero; that is, the point on the y-axis a distance $l_1 - l_2$ above

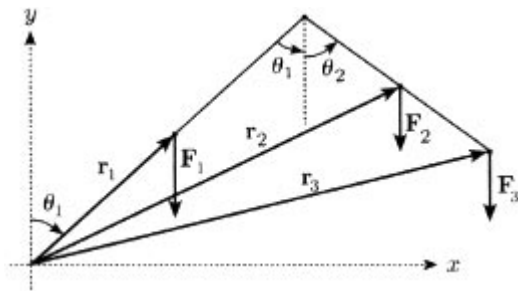


Figure 2. Free body diagram.

the primary joint O. The polar angles of the two shuttle arm segments, measured from the positive x -axis, are $(\pi/2) - \theta_1$ and $\theta_2 - (\pi/2)$, so the vectors to the points of application of the three forces are

$$\begin{aligned}\mathbf{r}_1 &= \frac{l_1}{2} \angle \left(\frac{\pi}{2} - \theta_1 \right) = \left(\frac{l_1}{2} \sin \theta_1 \right) \mathbf{i} + \left(\frac{l_1}{2} \cos \theta_1 \right) \mathbf{j}, \\ \mathbf{r}_2 &= 2\mathbf{r}_1 + \frac{l_2}{2} \angle \left(\theta_2 - \frac{\pi}{2} \right) = \left(l_1 \sin \theta_1 + \frac{l_2}{2} \sin \theta_2 \right) \mathbf{i} + \left(l_1 \cos \theta_1 - \frac{l_2}{2} \cos \theta_2 \right) \mathbf{j}, \\ \mathbf{r}_3 &= 2\mathbf{r}_1 + l_2 \angle \left(\theta_2 - \frac{\pi}{2} \right) = \left(l_1 \sin \theta_1 + l_2 \sin \theta_2 \right) \mathbf{i} + \left(l_1 \cos \theta_1 - l_2 \cos \theta_2 \right) \mathbf{j}.\end{aligned}$$

As the three forces are all parallel to \mathbf{j} , the x -components of the vectors \mathbf{r}_i make the only contribution to the cross products $\mathbf{r}_i \times \mathbf{F}_i$. Thus the torque of the robot arm and satellite about the primary joint O is

$$\begin{aligned}T_O(\theta_1, \theta_2) &= \sum \mathbf{r}_i \times \mathbf{F}_i \\ &= -a \left[\left(m_1 \frac{l_1}{2} + m_2 l_1 + m_3 l_1 \right) \sin \theta_1 + \left(m_2 \frac{l_2}{2} + m_3 l_2 \right) \sin \theta_2 \right] \mathbf{k}.\end{aligned}$$

We will treat the torque as a scalar function,

$$T_O(\theta_1, \theta_2) = a \left[\left(m_1 \frac{l_1}{2} + m_2 l_1 + m_3 l_1 \right) \sin \theta_1 + \left(m_2 \frac{l_2}{2} + m_3 l_2 \right) \sin \theta_2 \right]. \quad (1)$$

Typical configurations of the arm result in clockwise torques, which by convention are negative. We change the sign in defining the scalar torque function (1) so that now *clockwise torques yield positive values of $T_O(\theta_1, \theta_2)$* .

Single Variable Results

Initially we will suppose that the robot arm is geared so as to keep angles θ_1 and θ_2 equal. Once we understand this simplified model, which can be analyzed without calculus, we will remove the equal angle restriction to get a more interesting and realistic multivariable model.

We first determine the *workspace* of the robot arm; that is, the planer region that the tip of the arm can reach, ignoring any constraint from a torque restriction. Since the vector \mathbf{r}_3 describes the location of the tip of the robot arm, when $\theta_2 = \theta_1$ the workspace is simply the curve

$$\mathbf{r}_3(\theta_1) = (l_1 + l_2) \sin \theta_1 \mathbf{i} + (l_1 - l_2) \cos \theta_1 \mathbf{j}, \quad \text{for } 0 \leq \theta_1 \leq \frac{\pi}{2}.$$

This is the upper right quarter of the ellipse with center at the origin, horizontal semimajor axis of length $l_1 + l_2$, and semiminor axis of length $l_1 - l_2$, shown in Figure 3.

The expression (1) for the torque reduces, when $\theta_2 = \theta_1$, to

$$T_O(\theta_1) = a \left[m_1 \frac{l_1}{2} + m_2 \left(l_1 + \frac{l_2}{2} \right) + m_3 (l_1 + l_2) \right] \sin \theta_1. \quad (2)$$

Since $\sin \theta_1$ is nonnegative for $0 \leq \theta_1 \leq \pi/2$, this torque function will always be positive.

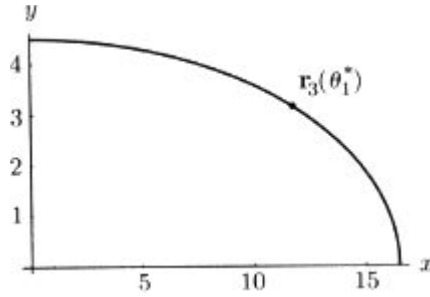


Figure 3. Workspace in single-variable model.

From what points in the workspace can a satellite be recovered while satisfying a torque restriction $T_O \leq T_{\max}$? Using the fact that the magnitude of the torque (2) is an increasing function of θ_1 for $0 \leq \theta_1 \leq \pi/2$, we see that if $T_O(\pi/2) \leq T_{\max}$ then the torque will never exceed the value T_{\max} . But if $T_O(\pi/2) > T_{\max}$, then the equation $T_O(\theta_1) = T_{\max}$ has a single root θ_1^* in the interval $0 \leq \theta_1 \leq \pi/2$. In this case the satellite can be snagged by the robot arm anywhere in the interval $0 \leq \theta_1 \leq \theta_1^*$ without violating the torque restriction.

Once the satellite has been grasped, it must be moved to the shuttle bay. We assume that the satellite has been snagged at the maximum admissible angle, $\theta_1 = \theta_1^*$. Then the directions for returning are given by the vector \mathbf{r}_3 : simply reverse the motion that extended the robot arm to the required angle θ_1^* , starting from its “docked” position at the shuttle bay. The resulting docking path, with parametric equations

$$\begin{aligned} x(\theta) &= (l_1 + l_2) \sin(\theta_1^* - \theta), \\ y(\theta) &= (l_1 - l_2) \cos(\theta_1^* - \theta), \end{aligned} \quad \text{where } 0 \leq \theta \leq \theta_1^*,$$

reduces the torque on the primary joint from its value $T_O(\theta_1) \leq T_{\max}$, at the moment when the satellite is grasped, to zero at the shuttle bay. The return path is part of Figure 3, starting at the position labeled $\mathbf{r}_3(\theta_1^*)$. Here, $T_{\max} = 800 \text{ N} \cdot \text{m}$, which leads to the root $\theta_1^* \approx 0.7938$.

The distance from the shuttle to the satellite for any angle $\theta_2 = \theta_1$ is easily computed by vector methods:

$$|\mathbf{r}_3(\theta_1)| = \sqrt{l_1^2 + l_2^2 - 2l_1l_2 \cos 2\theta_1}.$$

In other words, calculating the distance of the tip of the robot arm as the sum of the vectors along its two segments gives a constructive proof of the law of cosines! (See Figure 2 for the positions of the sides of the triangle.)

Multivariable Extensions

In the actual robot arm the angles θ_1 and θ_2 are independent of each other, but we will still maintain the previous angular constraints. The extra degree of freedom in the robot arm gives the pilot much more flexibility in maneuvering, so the analysis of the arm motion is considerably more sophisticated. The questions are the same as before: What is the workspace of the robot arm? What is the region from which a satellite can be

grasped and returned to the shuttle bay without violating a torque restriction $T_O \leq T_{\max}$? What is the optimal docking path—the path followed by the tip of the robot arm that leads from an accessible point back to the shuttle bay and decreases the torque on the primary joint most rapidly? A number of concepts from multivariable calculus give answers to these questions.

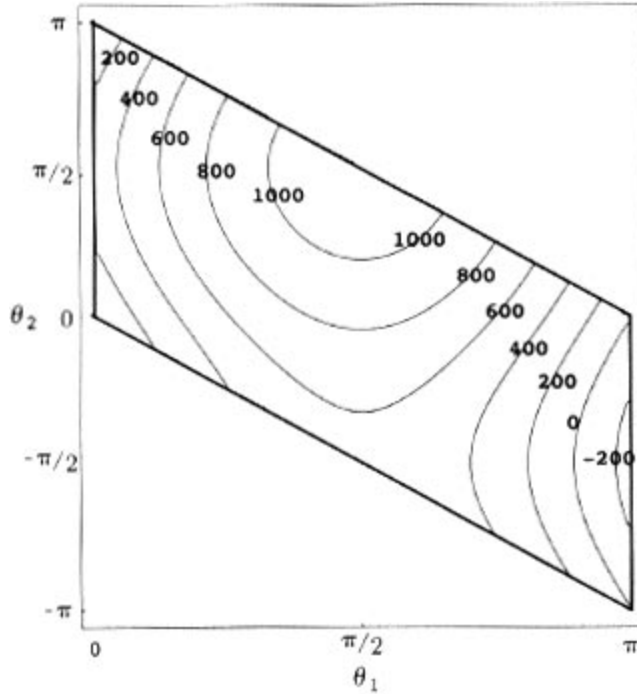


Figure 4

First let's examine the workspace of the robot arm—the region that the arm can reach. In the $\theta_1\theta_2$ -plane, the workspace is the region $0 \leq \theta_1 \leq \pi$ and $0 \leq \theta_1 + \theta_2 \leq \pi$; see Figure 4, where for later reference we also show the contours of the torque function (1) in this region. In the xy -plane containing the shuttle, robot arm, and satellite, the workspace will be the image of $\mathbf{r}_3(\theta_1, \theta_2) = (l_1 \sin\theta_1 + l_2 \sin\theta_2)\mathbf{i} + (l_1 \cos\theta_1 - l_2 \cos\theta_2)\mathbf{j}$ as (θ_1, θ_2) ranges over the region in Figure 4. This is Figure 5.

$$K_1 \sin\theta_1 + K_2 \sin\theta_2 = T_{\max}.$$

This system can be solved explicitly, but the solutions must be interpreted carefully because they depend on so many parameters. The first and second equations imply that either $\lambda = 0$ and $K_1 \cos\theta_1 = K_2 \cos\theta_2$. The case $\lambda = 0$ yields $\sin(\theta_1 + \theta_2) = 0$, so it corresponds to the solutions $\theta_1 + \theta_2 = \pi$ (the arm fully extended, maximum reach) or $\theta_1 + \theta_2 = 0$ (the short arm fully retracted, minimum reach). Using these linear relations and the constraint equation $K_1 \sin\theta_1 + K_2 \sin\theta_2 = T_{\max}$, we can solve explicitly for θ_1 and θ_2 . For values of T_{\max} larger than $K_1 + K_2$, there will be no solutions, of course. But for values of T_{\max} somewhat smaller than $K_1 + K_2$, there will be one solution with θ_1 an acute angle and a second solution with θ_1 equal to the supplementary angle.

Figure 6 shows a typical example. The solid curve shows all possible positions of $\mathbf{r}_3(\theta_1, \theta_2)$ of the tip of the robot arm for which the torque on the primary joint is $800 \text{ N} \cdot \text{m}$, and the dashed lines are contours of the distance function. There are three places along the torque contour that satisfy the Lagrange condition—places where the torque contour is tangent to the distance contour. One is in the middle of the torque contour. This is the point on the constant-torque curve with *minimum* reach of the robot arm, and it corresponds to a solution of Lagrange's equations with $K_1 \cos\theta_1 = K_2 \cos\theta_2$. The other two places are at the ends of the constant torque curve. They are tangent to the circle of maximum extension (radius $l_1 + l_2$) which is the image under the mapping \mathbf{r}_3 of the line $\theta_1 + \theta_2 = \pi$.

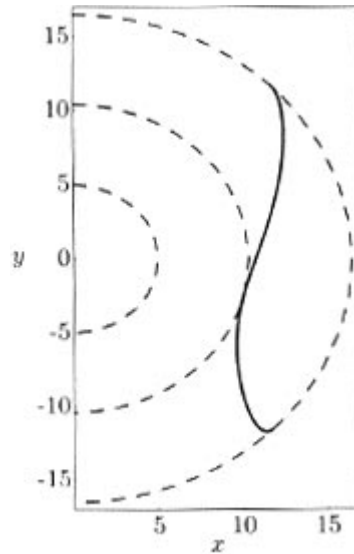


Figure 6. Path of the arm's tip ($T_{\max} = 800 \text{ N} \cdot \text{m}$).

Moreover, the ends of this constant-torque curve, the points of tangency, have equal x -coordinates. To see why, we use the identities $\sin(\pi - \theta) = \sin \theta$ and $\cos(\pi - \theta) = -\cos \theta$ and restrict our attention to the boundary line $\theta_1 + \theta_2 = \pi$. Along this line, $T_O = (\theta_1, \pi - \theta_1) = T_O(\pi - \theta_1, \theta_1)$; that is, the torque function restricted to the boundary line is symmetric about its midpoint, $(\pi/2, \pi/2)$. Similarly, we note that the x -coordinates of $\mathbf{r}_3(\theta_1, \pi - \theta_1)$ and $\mathbf{r}_3(\pi - \theta_1, \theta_1)$ agree, whereas the y -coordinates differ by a sign. Thus the two endpoints of a curve of constant torque (both of which lie on the line $\theta_1 + \theta_2 = \pi$) are mapped under \mathbf{r}_3 to points symmetric about the x -axis.

There continue to be three extremal values as T_{\max} decreases, until T_{\max} reaches $K_1 - K_2$. This is the torque value for which the minimum distance between the primary joint and the tip of the arm equals $l_1 - l_2$, the smallest possible reach of the robot arm, with the long arm on the x -axis and the short arm fully retracted. For values of T_{\max} less than $K_1 - K_2$, the curves of torque T_{\max} break into two or three pieces, being obstructed by one or two of the semicircular boundaries of the workspace. In either case, the results are the same. The maximum reaches of the arm still occur with maximum extension of the arm. However, there are now two values of θ_1 that result in minimum reach, corresponding to full retraction of the arm. These two complementary values of θ_1 are the solutions of the Lagrange equations that satisfy $\theta_1 + \theta_2 = 0$, *not* $K_1 \cos\theta_1 = K_2 \cos\theta_2$. Figures 4 and 5 show several curves of constant torque drawn on the workspace of the robot arm. The curve of torque $800 \text{ N} \cdot \text{m}$, for example, is seen in either case to have a single component, while the curves of constant torques $400 \text{ N} \cdot \text{m}$ and $200 \text{ N} \cdot \text{m}$ have two and three components, respectively. Note also that there are curves of constant negative torque, corresponding to positions of the robot arm, with $\theta_1 \approx \pi$ and negative values for angle θ_2 . Can you picture the corresponding positions of the robot arms and see physically why they yield counterclockwise torques about the primary joint? (Recall that the total torque about O is the same as if all the mass of the robot arm and satellite were located at the center of mass of the entire configuration.)

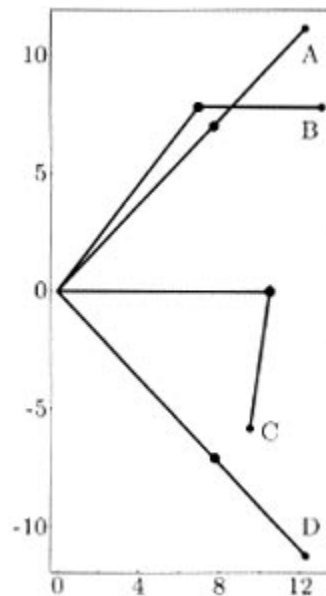


Figure 7. Four arm positions ($T_{\max} = 800 \text{ N} \cdot \text{m}$).

The analytic description of the path of the robot arm's tip as it traces a curve of constant torque provides insight into the accompanying motion of the arm's two segments. Consider how both segments move as the robot arm transports a satellite along a curve $T_O(x, y) = T$, for example, the curve of constant torque in Figure 6. Imagine the arm initially fully extended upwards, so $(\theta_1, \theta_2) = (0, \pi)$ and the torque is initially zero. If the arm rotates clockwise in the fully extended position, the torque T_O will increase until at some point A (Figure 7) it equals the value T of interest. As we see from Figure 4, this point of maximal reach of the robot arm will be on the boundary line $\theta_1 + \theta_2 = \pi$, and substituting into the constant-torque equation gives

$$K_1 \sin\theta_1 + K_2 \sin(\pi - \theta_1) = T,$$

so

$$\theta_1 = \arcsin\left(\frac{Y}{K_1 + K_2}\right).$$

(Thus, point A is $\mathbf{r}_3(\theta_1, \pi - \theta_1) \approx (11.765, 11.56)$ in Figure 6.) In order for the arm to move beyond this point while maintaining the same torque, the long inner segment must turn counterclockwise while the short outer segment rotates clockwise (compare to Figure 4). This will be the case until the arm reaches position B, where

$$\theta_2 = \frac{\pi}{2} \quad \text{and} \quad \theta_1 = \arcsin\left(\frac{T - K_2}{K_1}\right).$$

Then both segments of the arm turn clockwise in order to maintain the same torque, until point C, where $\theta_1 = \pi/2$. From here, the short segment rotates counterclockwise as the long segment continues clockwise until the arm is fully extended at D, where

$$\theta_1 = \pi - \arcsin\left(\frac{T}{K_1 + K_2}\right)$$

as expected.

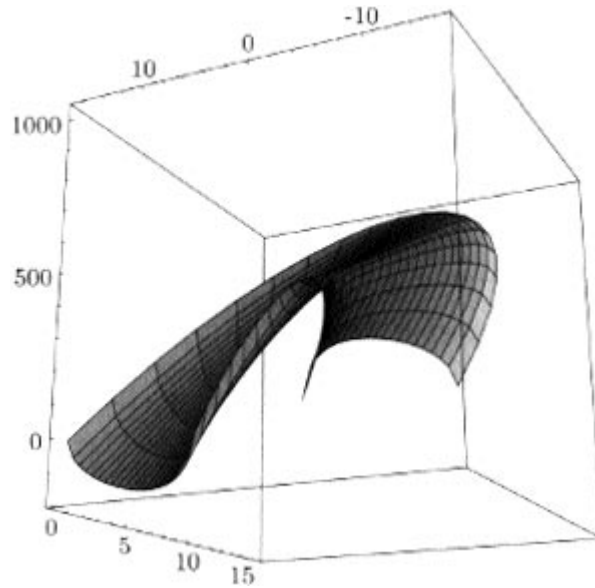


Figure 8. Graph of torque as a function of position.

We used this kind of analysis and the contours in the $\theta_1\theta_2$ -plane (Figure 4) to assist in plotting the contour curves in the xy -plane as in Figure 5. At this point we also include Figure 8, the three-dimensional graph of the torque as a function of position. We leave the construction of the graph as an exercise for the interested reader.

Docking Paths

At this stage we know a lot about how the robot's arm position and torque are related,

but having snagged the satellite the pilot still has the task of returning the arm to the shuttle bay without exceeding a given torque limit T_{\max} . What is the best path to follow? With a little prodding a calculus student might respond that the optimal path is to “follow the gradient” to reduce torque most quickly. The gradient vector $\nabla T_O(\theta_1, \theta_2)$ is perpendicular to the level curves, or curves of constant torque, and we can sketch on Figure 4 the orthogonal trajectory of the level curves that begins at any point in the domain. For a starting point (θ_1, θ_2) with $\theta_1 > \pi/2$, the path following $-\nabla T_O$ curves down and to the right in Figure 4 until it strikes the boundary line $\theta_1 = \pi$. Then it proceeds vertically to the midpoint of this edge, $(\pi, -\pi/2)$, and stops at this global minimum of the torque. Similarly, we see that for a starting point (θ_1, θ_2) with $\theta_2 > \pi/2$, the path following $-\nabla T_O$ curves up and to the left in Figure 4 until it strikes the boundary line $\theta_1 = 0$, whereupon it moves upward to end at $(0, \pi)$, a local minimum of the torque.

In neither of these cases does the strategy of following the gradient lead to the desired destination, the shuttle bay, which is also seen from Figure 4 to be a local minimum of the torque. However, for starting points (θ_1, θ_2) with $\theta_1, \theta_2 < \pi/2$ it is clear from the figure that the path following $-\nabla T_O$ will curve downward, decreasing both θ_1 and θ_2 until it hits either $\theta_1 = 0$ or $\theta_1 + \theta_2 = 0$, and thereafter it will follow this boundary line to the shuttle bay, where both angles are zero. For such starting points (θ_1, θ_2) , following the gradient will be the optimal strategy. But which paths lead to the boundary $\theta_1 = 0$

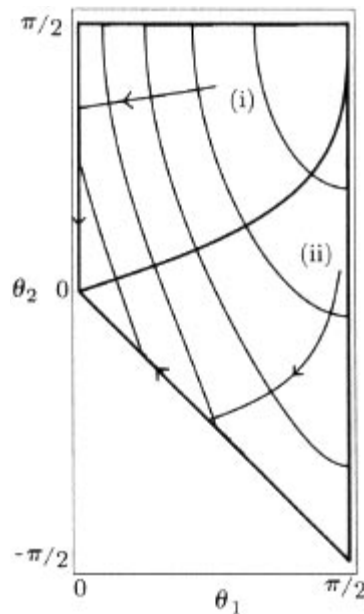


Figure 9. Optimal return paths.

and which lead to $\theta_1 + \theta_2 = 0$? Let’s call these two kinds of path types (i) and (ii); an example of each is shown in Figure 9.

The two types of path partition the restricted domain $\theta_1, \theta_2 < \pi/2$ into two regions, according to whether following the gradient from (θ_1, θ_2) to the origin is a path of type (i) or (ii). We are interested in the boundary between these two regions. This separating curve is a path following $-\nabla T_O$ that leads directly to the shuttle bay at the origin,

simultaneously meeting the two boundary lines $\theta_1 = 0$ and $\theta_1 + \theta_2 = 0$ there. To find it, we can just reverse the path and follow the gradient $+\nabla T_O$ from the origin and see where it leads!

We want a path $(\theta_1(t), \theta_2(t))$ for which the tangent vector $(\theta_1'(t), \theta_2'(t))$ will be a positive multiple of the gradient vector $\nabla T_O = K_1 \cos\theta_1(t)\mathbf{i} + K_2 \cos\theta_2(t)\mathbf{j}$. Taking this arbitrary multiple to be 1, we wish to solve the initial value problem

$$\begin{aligned} \theta_1'(t) &= K_1 \cos\theta_1(t), \\ \theta_2'(t) &= K_2 \cos\theta_2(t), \end{aligned} \quad \text{where } (\theta_1(0), \theta_2(0)) = (0, 0). \quad (3)$$

The equations are uncoupled, so all that is required is to integrate them separately.

Alternatively, dividing to eliminate the dependence on t , we get the single autonomous equation

$$\frac{d\theta_2}{d\theta_1} = \frac{K_2 \cos\theta_2}{K_1 \cos\theta_1}.$$

Separating variables and using the little-known trigonometric identity $\sec\theta + \tan\theta = \cot((\pi/4) - (\theta/2))$ we can solve explicitly for θ_2 :

$$\theta_2 = \frac{\pi}{2} - 2 \tan^{-1} \left\{ \frac{1}{C} \left[\tan\left(\frac{\pi}{4} - \frac{\theta_1}{2}\right) \right]^K \right\},$$

where C is an integration constant and $K = K_2/K_1$. Using the initial condition $\theta_2(0) = 0$ gives $C = 1$. Whether we solve the initial value problem numerically or in closed form, the graph of the solution curve separating the two regions is as indicated in Figure 9. If the satellite is retrieved at a point (θ_1, θ_2) on a type (i) path, the robot arm operator will rotate the long segment counterclockwise and the short segment clockwise, decreasing the two angles at rates specified by the differential equations (3), until the long segment is vertical ($\theta_1 = 0$). Then the short segment continues retracting (turning clockwise) until the satellite at its tip reaches the bay. If the starting point is in the other region, can you describe the motion of the two arms as the robot arm returns the satellite to the shuttle bay along a type (ii) path?

The problem of finding the best docking path may not be important for a single satellite retrieval, but it does have applications elsewhere. For example, in an automated assembly line a robot may perform identical motions hundreds or thousands of times a day. Any reduction in the stress on a joint will extend the life of the machine and reduce the cost of required maintenance.

Further Extensions

One factor we have ignored is dependence on time, and a full-scale analysis would have to take angular momentum into account. However the dynamic approach is more complicated than the static model. Our simplifications make this project appropriate for a multivariable calculus course. We guide our students through the single-variable results in this article and use the contour graph of the torque (Figure 4) to demonstrate the need for functions of two variables. The students find the project challenging, and many say it

is their key to understanding both the mathematical and the physical ideas. The torque analysis becomes an archetypal problem to which we often refer in motivating new material.

Our analysis by no means exhausts the problem, and interested readers might want to try their hand at extending some of our results. For instance:

Exercise 1. Using Figure 4, propose a good docking strategy for initial points with $\theta_1 \geq \pi/2$ and $\theta_2 \geq \pi/2$. Discuss its practical advantages and disadvantages.

Exercise 2. How does the motion of the arm change if the restriction on the angle θ_2 is removed, so that the smaller arm is allowed to make a full revolution?

Exercise 3. Say the angles of the arm are geared in a ratio of $n : m$, with n and m integers. Given a satellite retrieval point, how does the torque change as the arm starts to move? (Think *directional derivatives*.)

Exercise 4. Suppose a third segment, of length $l_1 - l_2$, is added to the robot arm to increase its range of motion. How will this affect the workspace? Note that a given retrieval point may have many different allowable configurations of the arm's segments. What will the regions of constant torque look like? How will the three segments move as the tip of the robot arm traverses a curve of constant torque?

Exercise 5. Add another segment as above and consider the arm as a system with three degrees of freedom. What do the level surfaces look like? Discuss optimal docking strategies.

Acknowledgment. We thank the referees for their many helpful comments and suggestions.